Molecular Crystals and Liquid Crystals

Publication details, including instructions for authors and subscription information:
http://www.tandfonline.com/loi/gmcl20

Optical Properties of Nanoimprinted Grating with Nematic Liquid Crystal

Ryotaro Ozaki [a], Toshikazu Shinpo [a], Hiroshi Moritake [a], Katsumi Yoshino [b] & Masanori Ozaki [c]

[a] Department of Electrical and Electronic Engineering, National Defense Academy, Yokosuka, Kanagawa, Japan

[b] Shimane Institute for Industrial Technology, Matsue, Shimane, Japan

[c] Division of Electrical, Electronic and Information Engineering, Graduate School of Engineering, Osaka University, Suita, Osaka, Japan

Version of record first published: 05 Oct 2009

To cite this article: Ryotaro Ozaki, Toshikazu Shinpo, Hiroshi Moritake, Katsumi Yoshino & Masanori Ozaki (2009): Optical Properties of Nanoimprinted Grating with Nematic Liquid Crystal, Molecular Crystals and Liquid Crystals, 507:1, 234-244

To link to this article: http://dx.doi.org/10.1080/15421400903051424

Mol. Cryst. Liq. Cryst., Vol. 507, pp. 234–244, 2009

ISSN: 1542-1406 print/1563-5287 online
DOI: 10.1080/15421400903051424

Taylor & Francis
Taylor & Francis Group

Optical Properties of Nanoimprinted Grating with Nematic Liquid Crystal

Ryotaro Ozaki[1], Toshikazu Shinpo[1], Hiroshi Moritake[1], Katsumi Yoshino[2], and Masanori Ozaki[3]
[1]Department of Electrical and Electronic Engineering, National Defense Academy, Yokosuka, Kanagawa, Japan
[2]Shimane Institute for Industrial Technology, Matsue, Shimane, Japan
[3]Division of Electrical, Electronic and Information Engineering, Graduate School of Engineering, Osaka University, Suita, Osaka, Japan

We study optical properties of nanoimprinted gratings infiltrated with liquid crystal (LC). One-dimensional grating of a line-spacing pattern is used as a distributed feedback cavity. After filling LC into the trenches of the grating, the LC molecules align along the trench of grating and it shows uniform planar alignment. By optical pumping, laser emission occurs and the laser wavelength can be tuned by temperature control or application of voltage. We also demonstrate control of diffraction intensities from a two-dimensional grating using LC molecular reorientation in micro space.

Keywords: grating; laser; nanoimprint lithography; nematic liquid crystal

I. INTRODUCTION

Nanoimprint lithography (NIL), which is a novel method of nanopattern transfer, has been of considerable practical interest for low-cost technology and mass production [1]. In particular, NIL is well suitable for the fabrication of the nanoscale structure of polymer materials. The NIL technique is expected for development of nanofabrications of organic optical devices such as a flexible distributed feedback

The authors would like to acknowledge Merck KGaA and Sumitomo 3M for providing the nematic mixture and moldreleasing agent, respectively.

Address correspondence to Ryotaro Ozaki, Department of Electrical and Electronic Engineering, National Defense Academy, 1-10-20 Hashirimizu, Yokosuka, Kanagawa 239-8686, Japan. E-mail: ozaki@nda.ac.jp

(DFB) laser [2]. Micropatterns fabricated by NIL have been used not only as optical devices but also for the study of liquid crystal (LC) alignment, because the gratings play an important role in LC molecular alignment [3,4].

Photonic crystals (PCs) having a periodic structure with a periodicity equivalent to an optical wavelength have been studied by a number of investigators [5,6]. Since PCs have photonic band gaps (PBGs) in which photon propagation is forbidden. Using PBG, the developments of next generation optical devices, such as low-threshold lasers, microwaveguides, and micro-optical circuits, are expected. Tunable PCs having controllable photonic band gaps by varying optical periodicities are also expected for functional applications, for example, tunable lasers, optical switching, and tunable optical waveguides. In particular, PC infiltrated with LC has attracted considerable attention because LC has a large optical anisotropy and good sensitivities for electric filed, magnetic field, temperature, and so on [7–9]. Recently, we have reported a one-dimensional (1D) PC having a tunable nematic LC defect layer in which the wavelength of a defect mode can be controlled by applying an electric field [10]. We have also proposed a wavelength controllable laser and a fast optical switching [11–15]. Further, a wavelength controllable DFB laser has been demonstrated using a LC infiltrated DFB grating fabricated by NIL [16].

In this study, we investigate the optical properties of 1D and two-dimensional (2D) grating infiltrated with nematic LC. In 1D grating experiment, a line-spacing pattern DFB cavity is fabricated by UV-NIL, and the trench of the grating is filled with dye-doped nematic LC. Using this sample, we demonstrate tunable LC lasing by temperature control or application of electric field. We also demonstrate control of diffraction intensities from a 2D grating infiltrated with LC using molecular reorientation.

II. FABRICATION OF DEVICES

A schematic illustration of a nanoimprinted polymer grating infiltrated with LC is shown in Figure 1. To apply electric field, the grating and LC layer were sandwiched between two indium tin oxide (ITO)-coated glasses. The gratings were fabricated using nanoimprint molds of 1D line-spacing or 2D dot patterns. In this study, a 1D quartz nanoimprint mold had 100 nm line and 100 nm space pattern, and its pattern depth was also 100 nm. And we used a 2D quartz nanoimprint mold having dot patterns whose sizes are from 2 μm to 10 μm. The mold surfaces were coated with mold-releasing agent (EGC-1720, 3M) to easily detach the polymer grating.

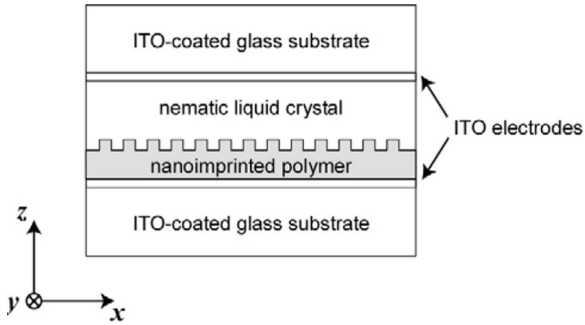

FIGURE 1 Schematic illustration of liquid-crystal/polymer grating fabricated by nanoimprint lithography.

The sandwich cell consisting of the quartz mold and the ITO coated glass was assembled using 25-μm poly(ethylene terephthalate) (PET) films as a spacer to uniform the thickness of the grating layer. The 25-μm gap was filled with a photopolymerized resin (PAK-01CL, Toyo Gosei), and then the sample was irradiated with UV light for 2 min. After polymerization, the mold was detached from the ITO glass. Since the surfaces and trenches of the mold were treated with the releasing agent, the mold was easily detached from the ITO-coated glass and replica. The scanning electron microscopy (SEM) images of the replicas of the mold patterns are shown in Figure 2. Figures 2(a) and 2(b) are the line-space pattern of 100 nm and hole patterns of 2-μm and 3-μm, respectively. The patterns of the polymer gratings conformed to the geometry of the molds.

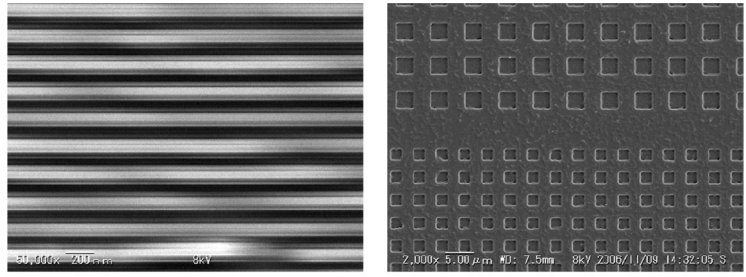

(a) (b)

FIGURE 2 SEM images of nanoimprinted gratings. (a) 100 nm line and spacing pattern. (b) 2-μm and 3-μm hole patterns.

After preparing replicas, we again assembled a sandwich structure using the ITO-coated glass with the polymer grating and another nonpatterned ITO-coated glass, as shown in Figure 1. PET films of 6 μm were used as a spacer. And then, a nematic LC mixture (E44, Merck) was infiltrated into the gap. Orientation treatment for LC on the glass surface describes in later section. We used a nematic LC (E44, Merck) whose ordinary and extraordinary refractive indices of the LC mixture are 1.53 and 1.78, respectively. In contrast, the polymer resin used as a grating has optical isotropy, and its refractive index is 1.53.

III. 1D GRATING WITH NEMATIC LIQUID CRYSTAL

In this section, we discuss a 1D grating with nematic LC as a tunable DFB laser. DFB lasers have been studied by many researchers since the first demonstration by Kogelnik *et al.* in 1971, because DFB structures are key components for optical devices and integrated optical circuits [17,18]. NIL enables to produce a grating structure with easy process.

Before discussing 1D grating infiltrated with LC, we discuss a laser action from a dye-doped 1D grating without LC. The grating used in this experiment is shown in Figure 2(a). To obtain laser emission, a dye (DCM, Exciton) was dopped in photopolymerized resin. The concentration of the dye was 0.5 wt%. As a pump source, a second-harmonic light of a Qswitched Nd:YAG laser was used, whose wavelength, pulse width, and pulse repetition frequency were 532 nm, 8 ns, and 10 Hz, respectively. The pump laser beam was focused by a spherical lens. The emission spectrum from the grating was measured using a charge-coupled device (CCD) multichannel spectrometer having a 2 nm wavelength resolution. The photodetector of the spectrometer was placed parallel to the x-axis corresponding to the periodic direction of the grating. Figure 3 shows the emission spectrum and photograph from the dye-doped 1D grating without LC. We obtained the narrow peak at 591 nm due to laser action. As is evident from Figure 3(b), the emission light propagates parallel to the periodicity of grating. These results indicate our grating has a good laser cavity.

To infiltrate LC into the trenches of a grating, we prepared a sandwich cell using the ITO-coated glass with grating and another nonpatterned ITO-coated glass, as mentioned earlier. The surface of the nonpatterned glass was coated with a polyimide film to align LC molecules, and then it was rubbed unidirectionally. The rubbing direction was parallel to the y-axis corresponding to the trench direction

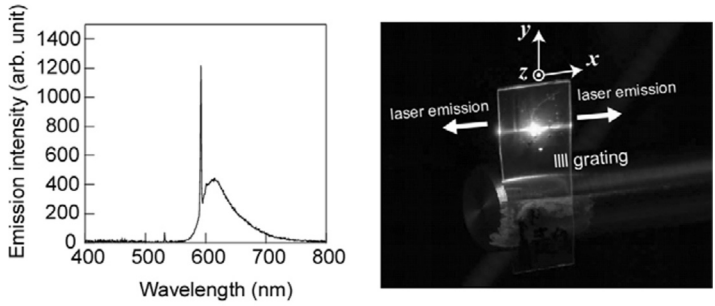

FIGURE 3 (a) Emission spectrum from a dye-doped polymer grating without LC. (b) Photograph of laser action from the dye-doped polymer grating.

of the polymer grating. In contrast, the ITO-coated glass with the polymer grating was not coated with a polyimide film and was not rubbed. Therefore, different surface alignment mechanisms are involved in this sample. The molecules on the nonpatterned glass and polymer grating are aligned by the rubbed polyimide film and the surface shape of the grating, respectively. After filling LC, we confirmed the planar texture of the sample by polarizing microscopy observation. Figure 4 shows the polarization microscopy images of the LC-filled grating. Figures 4(a) and 4(b) show dark and bright

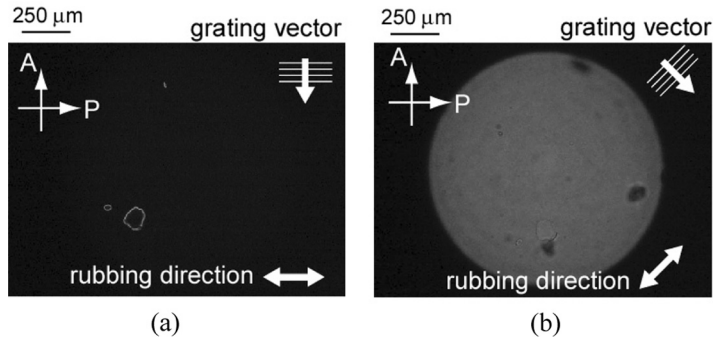

FIGURE 4 Polarization microscope images of 1D grating infiltrated with LC. The rubbing direction of the polyimide is parallel to trenches of polymer grating. The images (a) and (b) show dark and bright states under crossed nicols, respectively, which indicates that the LC director aligns along the rubbing and trench directions.

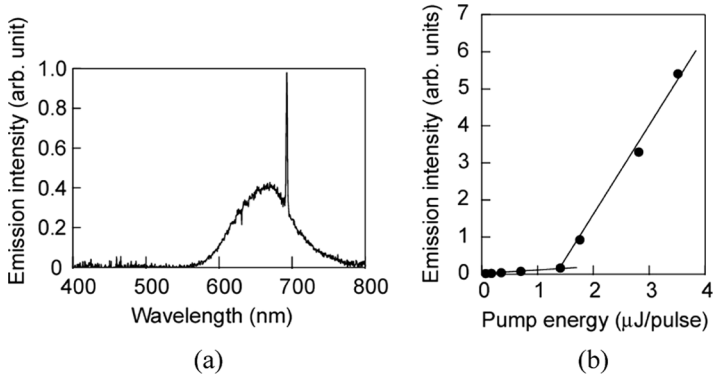

FIGURE 5 Emission spectrum from LC infiltrated grating at 1.76 μJ/pulse. (b) Pump energy dependence of the peak intensity at 698 nm.

states under crossed nicols, respectively, which indicates that the LC director is along the rubbing and trench directions.

Figure 5 shows emission spectrum and pump energy dependence of emission intensity of the sample. In this case, a laser dye (LDS-698, Exciton) was doped in nematic LC with 0.5 wt% because the resonance wavelength in the DFB cavity shifted to longer wavelength by filling LC into air space. The sample was pumped using the Qswitched Nd:YAG laser of 532 nm. The pump laser beam was focused by a cylindrical lens and the sample was irradiated with the beam from the LC layer side. The irradiation region was a stripe of approximately 50 μm × 5 mm. A broad emission from the sample is observed at a low pump energy. The emission spectrum having a 660 nm peak agrees with the spontaneous emission of the doped dye. By increasing the pump energy, a sharp peak appeared at 698 nm above a certain threshold energy. Figure 5(a) shows the emission spectrum at 1.76 μJ/pulse. Note that the wavelength of the sharp peak obviously differs from the peak wavelength of the spontaneous emission of the dye. The sharp peak wavelength indicates the long-wavelength edge of the stop band of the LC/polymer grating. The pump energy dependence of the emission intensity at 698 nm is shown in Figure 5(b). Above the threshold at a pump pulse energy of about 1.4 μJ, the emission intensity markedly increases. This indicates that there exists a lasing threshold above which light amplification accrues. The full-width at half-maximum of the sharp peak above the threshold is about 2 nm, which is limited by the spectral resolution of the CCD spectrometer used in this experiment. On the other hand, the broad spontaneous emission of the doped dye is only observed when the photodetector

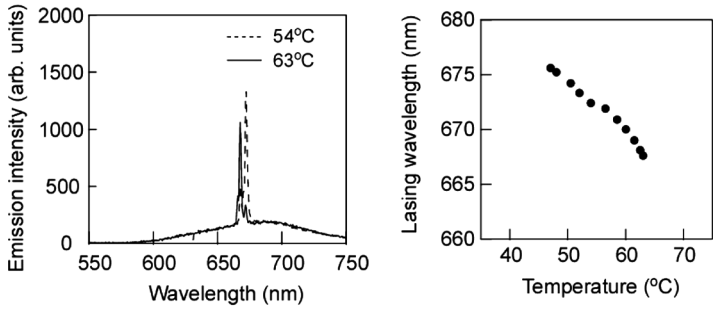

FIGURE 6 (a) Lasing spectra from LC infiltrated grating at 54°C and 63°C. (b) Temperature dependence of the lasing wavelength.

was placed along the *y*-axis which was perpendicular to the periodic direction. These results indicate that the enhanced light is due to the laser emission from the LC/polymer grating.

To achieve control of lasing wavelength, we attempted to change temperature of sample using a temperature controller system (FP82, Mettler). The dependence of lasing wavelength on temperature is shown in Figure 6. The sharp emission peak shifts to shorter wavelength with increasing temperature. As seen in Figure 6(b), the lasing wavelength is proportional to temperature. This peak shift is due to decrease of refractive index of LC with increase temperature.

Figure 7(a) shows the emission spectra from the LC/polymer grating for various voltages. To control the refractive index of the LC layer electrically, a rectangular voltage with a frequency of

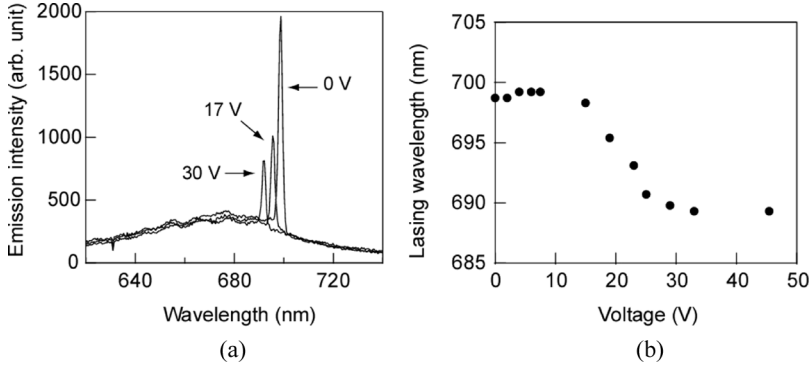

FIGURE 7 (a) Lasing spectra from LC infiltrated grating for various voltages. (b) Dependence of the lasing wavelength on applied voltage.

1 kHz was applied to the ITO electrodes. The sharp peak shifts to shorter wavelengths with increasing voltage, whereas the broad spontaneous emissions of the dye are unchanged. The peak shift is due to the molecular reorientation in the LC layer by voltage application. Before voltage application, the LC molecules in the trench of the polymer grating align in the trench direction, which corresponds to the *y*-axis. After voltage application, the molecules are reoriented from the *y*-axis to the *z*-axis. The molecules in the grating trench tilt slightly because they are anchored to the surface of the grating. Under this condition, the *y*-polarized light at the trench is affected by the polymer refractive index and an effective refractive index which is slightly smaller than the extraordinary index of LC. Therefore, the decrement in optical periodicity for the *y*-polarized light induces the lasing wavelength shifts to shorter wavelengths. On the other hand, the *z*-polarized light at the trench is affected by the polymer refractive index and another effective refractive index which is slightly larger than the ordinary index of LC. However, because the refraction contrast for the *z*-polarized light is still small, the *z*-polarized light is not associated with the laser emission.

The dependence of the lasing wavelength on the applied voltage is shown in Figure 7(b). A 10 nm shift is observed with an applied voltage of 30 V. With increasing voltage, the lasing spectrum begins to shift to shorter wavelengths at 10 V, which is associated with Frederiks transition. The Frederiks threshold is higher than that of an ordinary sandwich cell because the device consists of the 6 μm LC layer and the 25 μm polymer grating. Since the polymer grating has fourfold thickness in comparison with the LC layer, the effective voltage of the LC layer is approximately one-fifth of the total voltage. Furthermore, the threshold voltage indicates a molecular reorientation in the trench of the grating. Since the molecules in the trench are strongly anchored to grating walls, the threshold becomes higher than that of an ordinary sandwich cell.

IV. 2D GRATING WITH NEMATIC LIQUID CRYSTAL

Here we discuss about control molecular orientation in 2D pattern grating fabricated by UV-NIL. As mentioned earlier, the 2D replica has several hole sizes from 2 μm to 10 μm, and its depth is 350 nm. I prepared a sandwich cell using an ITO-coated glass with grating and another nonpatterned ITO-coated glass as the same manner as the 1D grating. After preparing sandwich cell, the nematic LC mixture was infiltrated into the gap. In this sample, the surface of the nonpatterned glass was coated with a polyimide film to align LC

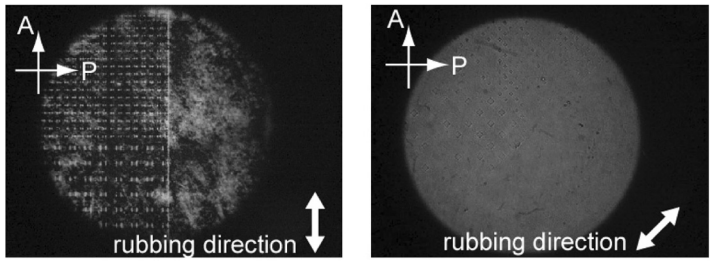

(a) (b)

FIGURE 8 Polarization microscope images of 2D grating infiltrated with LC. The images (a) and (b) show dark and bright states under crossed nicols, respectively.

molecules. Both 2D polymer grating and polyimide coated glass were rubbed unidirectionally parallel to the y-axis. Figure 8 shows polarization microscopy images of the sample. Figures 8(a) and 8(b) show dark and bright states under crossed nicols, respectively. The images show that the almost molecules align along the rubbing directions. However, the dark state of 2D grating is worse than that of 1D grating. We speculated that the tip of rubbing roll could not sufficiently rub in the hole.

Figure 9 shows diffraction patterns from LC infiltrated 2D gratings of (a) 10-μm, (b) 5-μm, and (c) 3-μm hole patterns. He-Ne laser was irradiated perpendicular to the grating pattern through a polarizer. The polarization of the incident beam is parallel to the molecular direction. The incident beam is affected by extraordinary refractive index 1.78 of LC and refractive index 1.53 of polymer resin. As seen in Figure 9, the distance of diffraction pattern d depends on the hole size. The distance d is determined by

$$d = \frac{\lambda}{n_{ave}\Lambda}L, \tag{1}$$

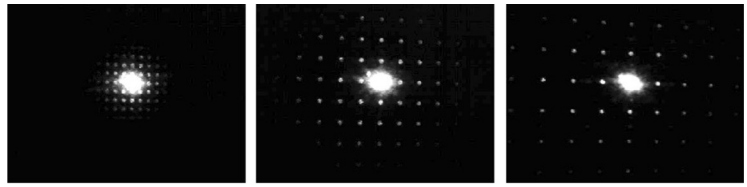

(a) 10 μm (b) 5 μm (c) 3 μm

FIGURE 9 Diffraction patterns from LC infiltrated 2D gratings of (a) 10-μm, (b) 5-μm, and (c) 3-μm hole patterns.

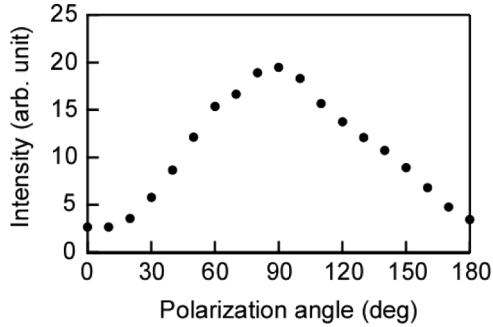

FIGURE 10 Polarization dependence of diffraction intensity from LC infiltrated 2D grating of 3-μm hole pattern.

where λ is wavelength of incident beam, n_{ave} is average index of grating, Λ is period of grating, L is distance between sample and screen. Each measured distances agree with calculation. On the other hand, we also examined the dependence of diffraction intensity on the polarization angle of the incident beam using photodiode. The polarization dependence of diffraction intensity from 3-μm hole pattern plotted in Figure 10. The intensity shows the maximum at 90 degree that corresponds to rubbing direction. The minimum is at 0 degree due to index matching. From this result, we also confirmed the LC molecules align the rubbing direction.

To control molecular orientation in 2D grating, a rectangular voltage of 10 V with a frequency of 1 kHz was applied to the ITO electrodes. Figures 11(a) and 11(b) show the diffraction patterns without and with the voltage, respectively. The diffraction pattern disappears by applying the voltage because the molecules are reoriented to z-axis. In this

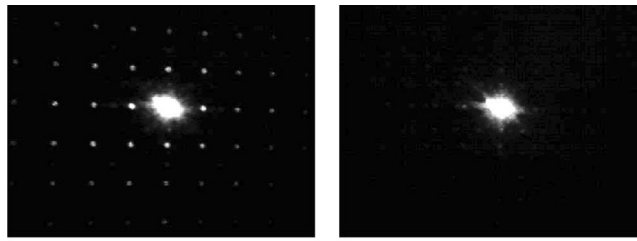

FIGURE 11 Diffraction patterns (a) without voltage and (b) with applied voltage of 10 V.

orientation, the incident beam is affected by ordinary index of LC and index of polymer resin. As is evident from this result, we were able to electrically control the molecular orientation in micro space.

V. CONCLUSION

We fabricated 1D and 2D gratings having submicron periodic structures by UV-NIL. The patterns of the imprinted gratings conformed to the exact geometry of the molds. To obtain uniform molecular alignment, we attempted orientation alignment before filling LC into the trench of the grating. The molecular orientations were able to control by orientation alignment. In 1D grating with LC, laser emission was observed upon the irradiation of pump laser beams above the threshold energy. Furthermore, we demonstrated a tunable laser by temperature control or application of voltage. In 2D grating with LC, we demonstrated the control of diffraction intensities from the grating using LC molecular reorientation in micro space.

REFERENCES

[1] Chou, S. Y., Krauss, P. R., & Renstrom, P. J. (1995). *Appl. Phys. Lett.*, *67*, 3114.
[2] Berggren, M., Dodabalapur, A., Slusher, R. E., Timko, A., & Nalamasu, O. (1998). *Appl. Phys. Lett.*, *72*, 410.
[3] Kim, Y.-T., Hwang, S., Hong, J.-H., & Lee, S.-D. (2006). *Appl. Phys. Lett.*, *89*, 173506.
[4] Yi, Y., Nakata, M., Martin, A. R., & Clark, N. A. (2007). *Appl. Phys. Lett.*, *90*, 163510.
[5] Yablonovitch, E. (1987). *Phys. Rev. Lett.*, *58*, 2059.
[6] John, S. (1987). *Phys. Rev. Lett.*, *58*, 2486.
[7] Yoshino, K., Shimoda, Y., Kawagishi, Y., Nakayama, K., & Ozaki, M. (1999). *Appl. Phys. Lett.*, *75*, 932.
[8] Busch, K. & John, S. (1999). *Phys. Rev. Lett.*, *83*, 967.
[9] Shimoda, Y., Ozaki, M., & Yoshino, K. (2001). *Appl. Phys. Lett.*, *79*, 3627.
[10] Ozaki, R., Matsui, T., Ozaki, M., & Yoshino, K. (2002). *Jpn. J. App. Phys.*, *41*, L1482.
[11] Ozaki, R., Matsui, T., Ozaki, M., & Yoshino, K. (2003). *Appl. Phys. Lett.*, *82*, 3593.
[12] Ozaki, R., Matsuhisa, Y., Ozaki, M., & Yoshino, K. (2004). *Appl. Phys. Lett.*, *84*, 1844.
[13] Ozaki, R., Ozaki, M., & Yoshino, K. (2003). *Jpn. J. App. Phys.*, *42*, L669.
[14] Ozaki, R., Moritake, H., Yoshino, K., & Ozaki, M. (2006). *J. App. Phys.*, *101*, 033503.
[15] Ozaki, R., Ozaki, M., & Yoshino, K. (2004). *Jpn. J. App. Phys.*, *43*, L1477.
[16] Ozaki, R., Shinpo, T., Yoshino, K., Ozaki, M., & Moritake, H. (2008). *Appl. Phys. Express.*, *1*, 012003.
[17] Kogelnik, H. & Shank, C. V. (1971). *Appl. Phys. Lett.*, *18*, 152.
[18] Kogelnik, H. & Shank, C. V. (1972). *J. Appl. Phys.*, *43*, 2327.